

## **PLUME-FREE STREAM INTERACTION HEATING EFFECTS**

### **DURING ORION CREW MODULE REENTRY**

Jeremiah J. Marichalar, Jacobs Technology – ESCG  
Forrest E. Lumpkin III, NASA Johnson Space Center  
Katie A. Boyles, NASA Johnson Space Center  
Houston, TX

### **ABSTRACT**

During reentry of the Orion Crew Module (CM), vehicle attitude control will be performed by firing reaction control system (RCS) thrusters. Due to the large scarf angles of the RCS thrusters and simultaneous firing of multiple thrusters, the simulation of the interaction of the RCS plumes with the oncoming flow has been difficult. The Orion aerothermodynamics database relies heavily on wind tunnel test data to capture the heating effects of thruster plume interactions with the free stream; however, this data is only valid for the continuum portion of the reentry trajectory. To extend the database to high altitudes during Orion CM reentry, a Direct Simulation Monte Carlo (DSMC) analysis was performed to study the vehicle heating effects resulting from the plume to free stream interaction. The study was performed with the DSMC Analysis Code using plume inflow boundary conditions obtained from Data Parallel Line Relaxation computational fluid dynamics solutions. Simulations were performed for the roll, yaw, pitch-up and pitch-down jets at altitudes of 105 km, 125 km and 160 km as well as vacuum conditions. Results show that the interaction effects decrease quickly with increasing altitude and are dependent on the thruster orientation with respect to the free stream and location on the vehicle.

### **INTRODUCTION**

The Orion Multi-Purpose Crew Vehicle (MPCV) will be the primary manned spaceflight vehicle of the National Aeronautics and Space Administration (NASA) mission for deep space exploration. Designed to be similar to the Apollo capsule, the MPCV Crew Module (CM) will serve as the crew return vehicle which brings astronauts safely back to the surface of the earth.

During the atmospheric reentry of the Orion CM, the vehicle will maintain attitude control by firing the reaction control system (RCS) thrusters. The CM surface heating caused by the interaction of the oncoming free stream with the plume exhaust flow field (termed jet/flow field interaction, or JFI) is a concern in developing the vehicle external thermal protection system (TPS). Historic Apollo flight reentry data<sup>1</sup> from heat rate sensors in the vicinity of the RCS thrusters show spikes in heat rate measurements that coincided with nearby RCS thruster firings. Fig. 1 displays the calorimeter flight data measurements from the Apollo 3 test flight along with the heat rate prediction based on laminar flow and the Reynolds number calculation (shown in the top region of the graph). The measurement data is difficult to decipher from the plot, and red arrows have been added to show the momentary heat flux increases from RCS thruster firings. The authors concluded that heat rate measurements during RCS thruster firings were as high as 5 times that measured between firings<sup>1</sup>. In order to account for the added heat load from RCS thruster firings, a substantial effort was made to develop a JFI heating model in the Orion aerothermodynamics database, which is used by vehicle manufacturers to size the TPS.

The Orion aerothermodynamics database has been developed from extensive analytical studies, high fidelity numerical simulations and ground testing. The high fidelity numerical simulations include both computational fluid dynamics (CFD) and Direct Simulation Monte Carlo (DSMC) solutions for vehicle reentry without active RCS firings (plume-off solutions). The JFI model for the Orion aerothermodynamics database relies heavily on wind tunnel test data to

capture the heating effects of thruster plume interactions with the free stream. Due to testing limitations, the wind tunnel test data is only valid for the continuum portion of the reentry trajectory. In order to extend the database JFI model to higher altitudes in the trajectory, a loosely coupled CFD/DSMC analysis<sup>2,3</sup> was performed to study the vehicle heating effects resulting from the JFI (plume-on solutions).

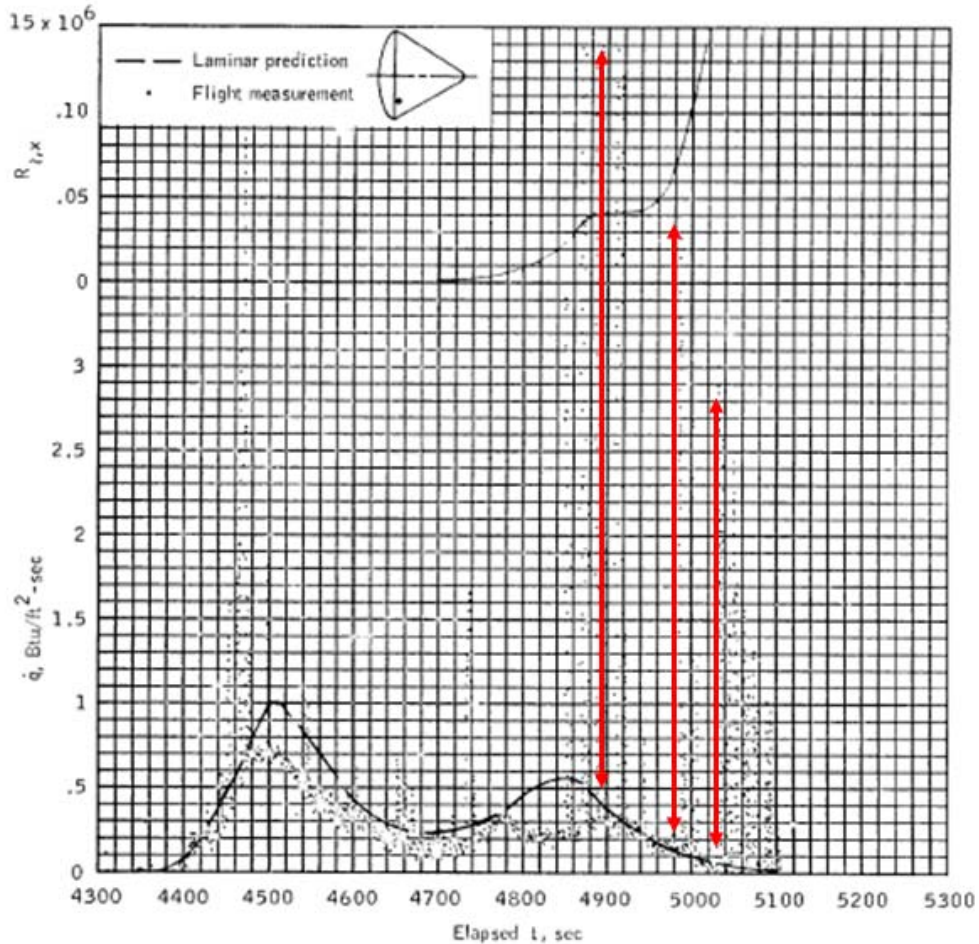


Figure 1. Heat transfer rate measurements obtained during Apollo 3 orbital entry.<sup>1</sup>

The remainder of this paper will discuss the methodology, assumptions, and the results of the CFD/DSMC simulations that were performed to capture the JFI heating effects for the Orion MPCV CM reentry trajectory.

### METHODOLOGY AND ASSUMPTIONS

Hybrid CFD/DSMC simulations have been used in past analyses to model rocket engine plume exhausts into the vacuum of space<sup>2,3,4</sup>. In the current analysis, a one-way coupled CFD/DSMC simulation is used to model the interaction of aft-vehicle, active RCS jet plumes with the oncoming free stream. The nozzle and near field continuum regions of the plume were modeled with the Data Parallel Line Relaxation (DPLR) CFD code<sup>5</sup>. The Bird continuum breakdown parameter<sup>6</sup> was computed for the CFD solution and a plume interface boundary well below the parameter value of 0.05 was defined. The inflow boundary conditions for the DSMC simulation were extracted from the CFD solution and interpolated to the plume interface (inflow) boundary. The DSMC Code (DAC)<sup>7</sup> was then used to simulate the expansion of the plume flow

field and the interaction with the oncoming rarefied free stream. The complexity of the simulation lies in the use of scarfed rocket engines and defining an appropriate interface boundary for the plume such that the interface geometry does not affect the oncoming free stream flow, supersonic inflow conditions at the interface are preserved, and computing the simulation does not become prohibitively expensive.

## GRID GENERATION

Commercial rocket engines are typically designed with axisymmetric nozzles, thus making the plume exhaust axisymmetric as well. Because the Orion CM outer mold line (OML) must remain unperturbed, the RCS thrusters are extended to be flush with the vehicle surface. This requirement significantly changes the rocket engine nozzle geometry and, therefore, the plume exhaust flow field. The nozzles for the Orion CM are called scarfed nozzles, which are typically defined by the scarf angle,  $\xi$  (shown in Fig. 2) between the scarfed nozzle exit plane and the exit plane of an ideal axisymmetric nozzle. Because of the asymmetry of scarfed nozzles, the simulations must be performed in three dimensions, which will increase grid generation and analysis complexity as well as simulation time. Due to the design of the Orion CM, some of the thrusters have large scarf angles, which will further increase simulation complexity.

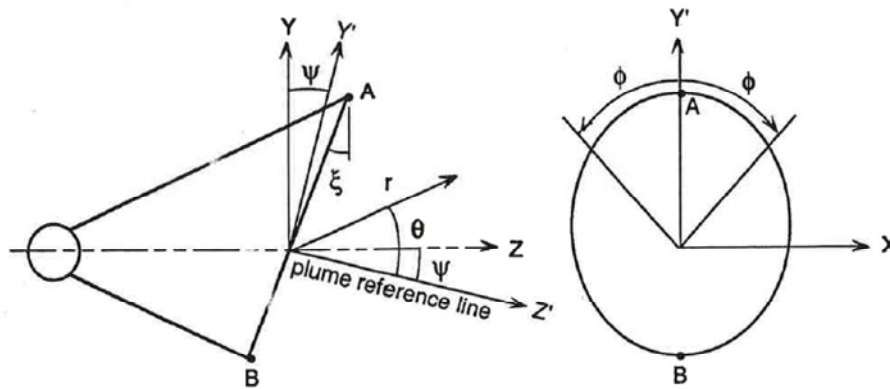


Figure 2. Schematic of a scarfed rocket engine nozzle.

A total of 12 thrusters exist on the Orion CM. Because of the symmetric placement of the thrusters, 4 distinct scarfed nozzles exist: the roll (A and B strings), yaw (A and B strings), pitch-down and pitch-up thrusters. Because of the scarf angle similarity and placement of the roll -A and -B jets and the yaw -A and -B jets, only the -B string thrusters were modeled in the full CFD/DSMC analysis. Dual jet firings were not considered in this study.

The generation of the three-dimensional, six-block structured grids for the DPLR simulations was performed with the GRIDGEN code developed by Pointwise, Inc. and the GridPro code developed by the Program Development Company. The automatic grid generation tools in the GridPro software make it well suited for creating good-quality, structured meshes within the confines of the complex 3D volume that occurs when modeling scarfed engine nozzles mounted flush with a vehicle surface. The nozzle and wall surface contours were created with the GRIDGEN software. The surfaces were then imported to GridPro, and the block structure and volume grids were created. Wall spacing was set to 10 microns, and wall-normal cell stretching was kept to 6% or less. A sample of the CFD geometry for the roll jet is shown in Fig. 3. The CFD meshes for the 4 scarf angle jets were all created with the same process.

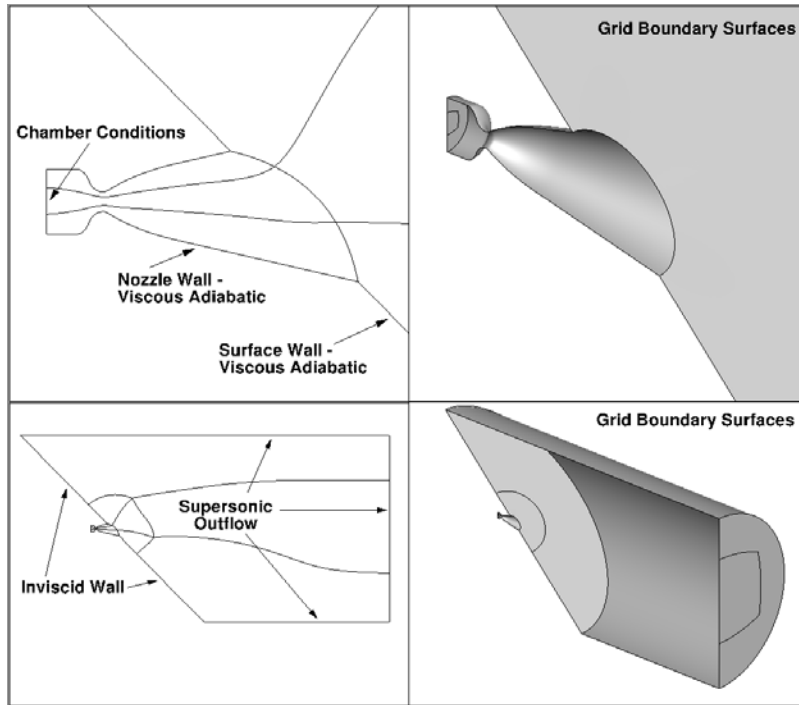


Figure 3. CFD grid geometry, topology and boundary conditions for roll jet DPLR simulation.

The unstructured grids for the DAC simulations were created with the GRIDGEN code. Each plume inflow boundary was created and attached to the Orion CM at the appropriate nozzle exit plane to complete a single water-tight surface for each single jet simulation. The final geometry for the vehicle and plume inflow boundary is shown in Fig. 4. The largest inflow boundary contains approximately 70,000 triangles while the Orion CM geometry contains approximately 100,000 triangles.

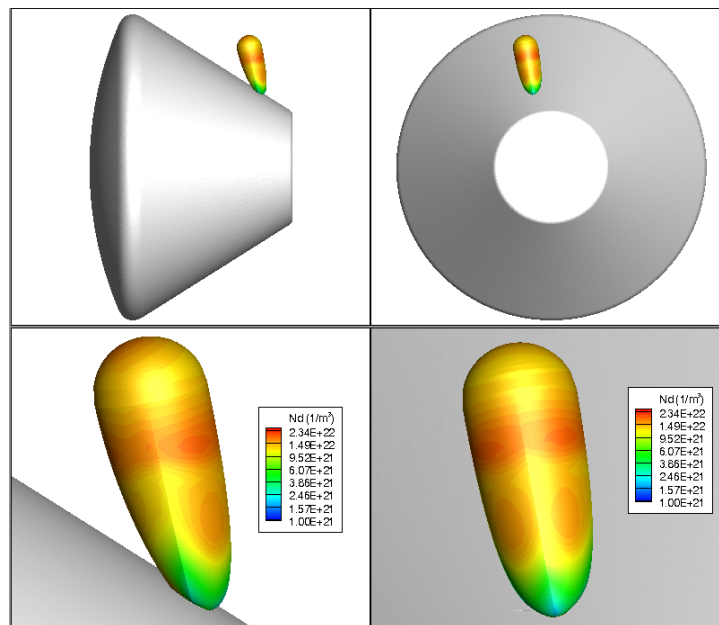


Figure 4. Final geometry for DAC simulation of pitch-down thruster firing from Orion CM.

## DPLR SIMULATIONS

The plume analysis begins in the continuum region with the steady-state CFD simulations of the rocket engine nozzle. For the current Orion MPCV design, Aerojet MR104 engines are used in the CM RCS. The MR104 is a mono-propellant hydrazine thruster that can produce approximately 100 lbf of thrust. The CFD simulations for these engines begin in the combustion chamber. The chamber pressure, chamber temperature and mass flow rate are defined by the engine manufacturer. The hydrazine gas is modeled with 7-species comprised mostly of nitrogen, hydrogen and ammonia. All of the simulations were assumed to be turbulent and used the shear stress transport (SST) two-equation turbulence model developed by Menter<sup>8</sup>. The purpose of the turbulence assumption is to ensure a conservative model (from the stand point of plume impingement heating) is incorporated into the Orion aerothermodynamic database. At a location downstream from the nozzle exit, chemical reactions and viscous terms are disabled. The viscous terms are disabled to keep the CFD solution from becoming unstable when conditions in the plume flow field become non-continuum. Chemical reactions are disabled because as the gas expands through the nozzle and into the plume, the temperature and pressure will drop to a point where the flow can be considered chemically frozen<sup>4</sup>. The engine is modeled as a typical conical combustion chamber with a convergent-divergent nozzle (see Fig. 3). Although the MR104 thruster inlet – which is designed with a catalyst bed over which the hydrazine gas passes – differs from the inlet modeled in the CFD simulation, the inlet area and velocity were adjusted to preserve the mass flow rate. An example of a completed plume solution can be seen in Fig. 5 which displays the pressure contours for the engine nozzle and near field plume region. Expansion waves emanate from both the sharp and shallow nozzle lips affecting the shape of the plume flow field. The plume cannot expand as far around the shallow nozzle lip as the sharp lip. As a result the plume is compressed between the expansion waves and the vehicle surface which causes a strong shock to occur. The asymmetric flow field structure that occurs in the near field region propagates outward into the far field plume regions as well.

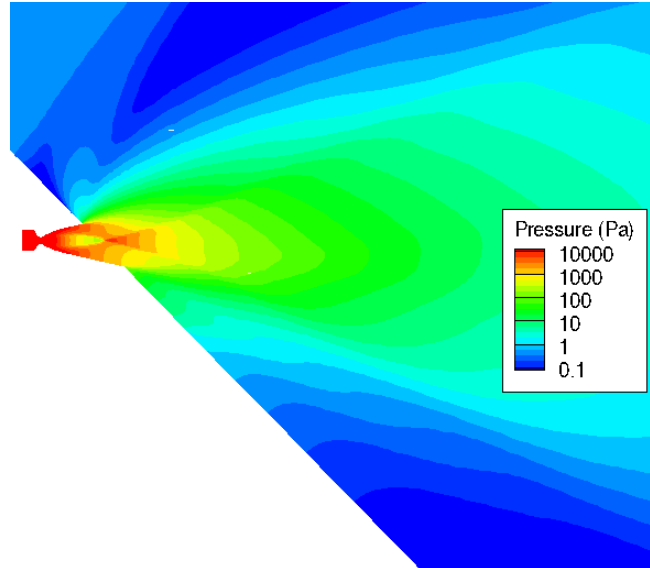


Figure 5. Pressure contours for DPLR simulation of Orion CM pitch-down thruster.

## PLUME INFLOW BOUNDARY

Once the CFD simulation of the nozzle and near-field plume flow reached steady-state, the plume inflow boundary was created for the DSMC simulation. The Bird breakdown parameter was computed and is shown in Fig. 6 for the pitch-down jet. The majority of the plume inflow boundary is well within the continuum flow field of the plume. The Bird parameter contours on the

inflow boundary show a maximum Bird value of 0.05 and a minimum value of 0.001 which is still within a manageable range for computational simulation with DAC. The plume inflow boundaries for all of the simulations were of a comparable size (approximately 10 nozzle radii in length and 3-4 nozzle radii in width). The final geometry for the vehicle and plume inflow boundary is shown in Fig. 4 with the number density contours for the inflow boundary displayed. The maximum number density in this case was  $2.5 \times 10^{22} \text{ m}^{-3}$ .

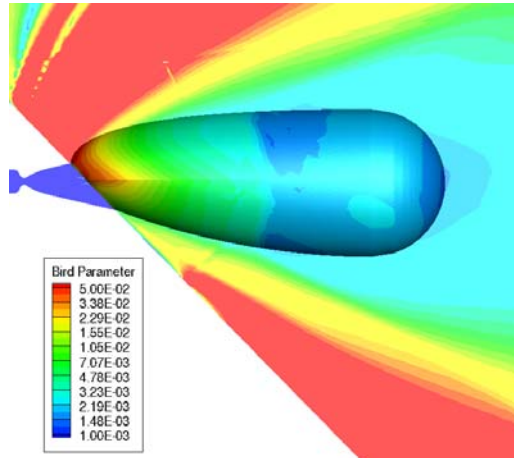


Figure 6. Bird breakdown parameter plotted for pitch-down thruster with superimposed inflow boundary used in the DAC simulations.

## DSMC SIMULATIONS

DAC steady state simulations were performed to model the continuum/rarefied regions of the plume including the interaction with the oncoming rarefied free stream. The gas file for the simulation used 6 species – 5 species air with a single specie RCS gas. The RCS gas has an effective molecular weight determined from the mixture of gases in the plume in the DPLR solution. This simplification was used because the plume exhaust is considered frozen in the CFD simulation. The first DAC simulation run for each jet was the vacuum plume solution with no free stream present. Then, simulations were run for 160 km, 125 km and 105 km altitudes with constant angle of attack and free stream velocity in order to match previous high altitude simulations in the MPCV Orion aero/aerothermodynamics database. A single adaption (mesh refinement) was used to further resolve the simulation and best practices DSMC plume modeling guidelines<sup>9</sup> were followed including using nearest neighbor collisions<sup>10</sup> which allows for relaxation of the standard 1.0 ratio of mean-free-path-to-cell-size resolution.

## **RESULTS AND DISCUSSION**

The remainder of this document will discuss the results and trends observed from the analysis of the JFI for the Orion MPCV CM. General solution characteristics, the plume/free stream flow field interaction, the interaction surface heating effects, and the solution quality will be discussed.

## COMPUTATIONAL RESOURCES

A total of 16 CFD/DSMC simulations were performed – four single jet firings for three database altitudes and vacuum conditions. The DPLR simulations of the nozzle and near field plume were completed on either 96 or 120 processors. For the DAC simulations, each free

stream case was performed on a minimum of 720 processors to complete the simulation in a reasonable amount of time, while the maximum number of processors used was 1800. For the vacuum cases, the number of processors ranged from 192 to 480. Table I shows the computational time (in CPU-hours per simulation time step) for each DAC simulation. In general, the lower free stream conditions (at 105 km and 125 km) required substantially more computational resources than the higher altitude and vacuum cases. The ratio of number density between the free stream and the plume for the lowest altitude simulation presented a computational challenge requiring 1800 cores of a parallel computer and approximately 2 billion representative molecules in order to meet simulation requirements.

Table I. Computational resource time for each simulation.

CASE	Roll	Yaw	Pitch Down	Pitch Up
105 km	0.73 cpu-hrs/step	0.19 cpu-hrs/step	0.33 cpu-hrs/step	0.55 cpu-hrs/step
125 km	0.16 cpu-hrs/step	0.10 cpu-hrs/step	0.48 cpu-hrs/step	0.88 cpu-hrs/step
160 km	0.14 cpu-hrs/step	0.10 cpu-hrs/step	0.19 cpu-hrs/step	0.15 cpu-hrs/step
Vacuum	0.26 cpu-hrs/step	0.11 cpu-hrs/step	0.09 cpu-hrs/step	0.11 cpu-hrs/step

### FLOW FIELD INTERACTION

A primary objective of this analysis was to use DAC to capture the high altitude plume/free stream interaction heating effects to the Orion vehicle surface. This effect can be seen in a side-by-side comparison of a JFI (plume-on) case and a database (plume-off) case as shown in Fig. 7 for the pitch-down jet. Fig. 7 displays the non-dimensional temperature contours in the flow field and the non-dimensional heat rate to the vehicle surface on similar scales for both (a) the plume-off and (b) the plume-on simulations. There is a clear increase in the surface heat rate not only in the near field region of the RCS nozzle but also in the far field region where the heating effects from the JFI can be observed. The pitch-down plume significantly changes the shape and flow field structure of the bow shock in front of the vehicle and causes JFI heating effects on the leeside shoulder. The temperature in the shock layer appears to be slightly lower in the plume-on simulation, but the 2-3% difference is in the statistical noise of the simulation. The non-dimensional heat rate values above the nominal 1.0 in the plume-on simulation indicate that the total energy of the plume is larger than that of the free stream.

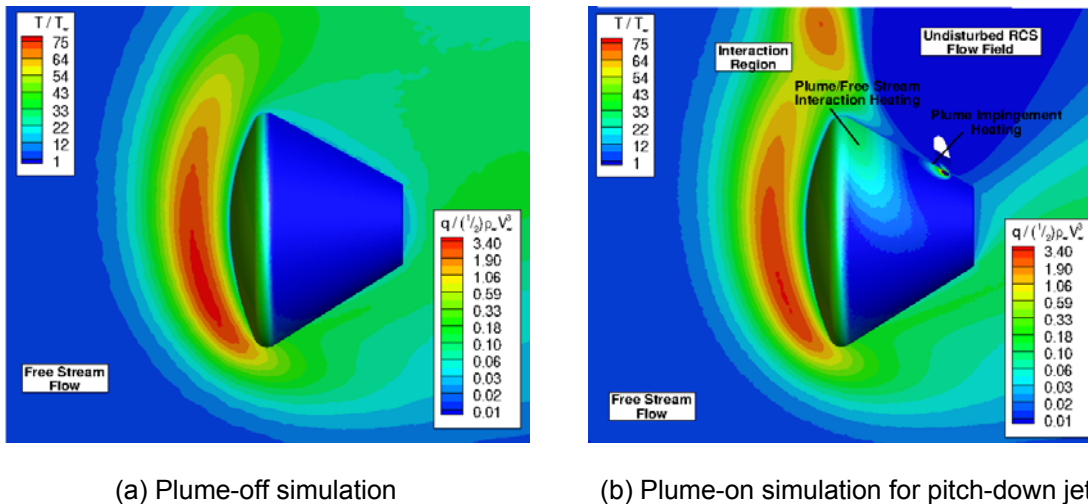


Figure 7. Flow field temperature contours and surface heat rates for Orion CM pitch-down jet at altitude of 105 km.

## SURFACE HEATING

The increase in surface heat rate caused by the JFI is one of the primary interests of vehicle TPS designers. The effects of the JFI and plume impingement on the vehicle surface heating as a function of altitude can be seen in Fig. 8. The plots show the delta increase in heat flux over the plume-off database solution on the same scale for each free stream condition. Because no database solution exists for the vacuum condition, the absolute heat flux is shown in Fig. 8 (d). The 105 km case in Fig.8 (a) shows a clear far field interaction region that is separate from the plume impingement near field region. The interaction region shrinks significantly in the 125 km case. The surface heating to the vehicle at 160 km is completely dominated by the plume flow field, and JFI heating effects are no longer present. The maximum JFI delta heat rate (less than  $1.0 \text{ W/cm}^2$ ) occurs in the 105 km case. The simulations for the roll, yaw and pitch-up jets yielded similar trends as a function of altitude.

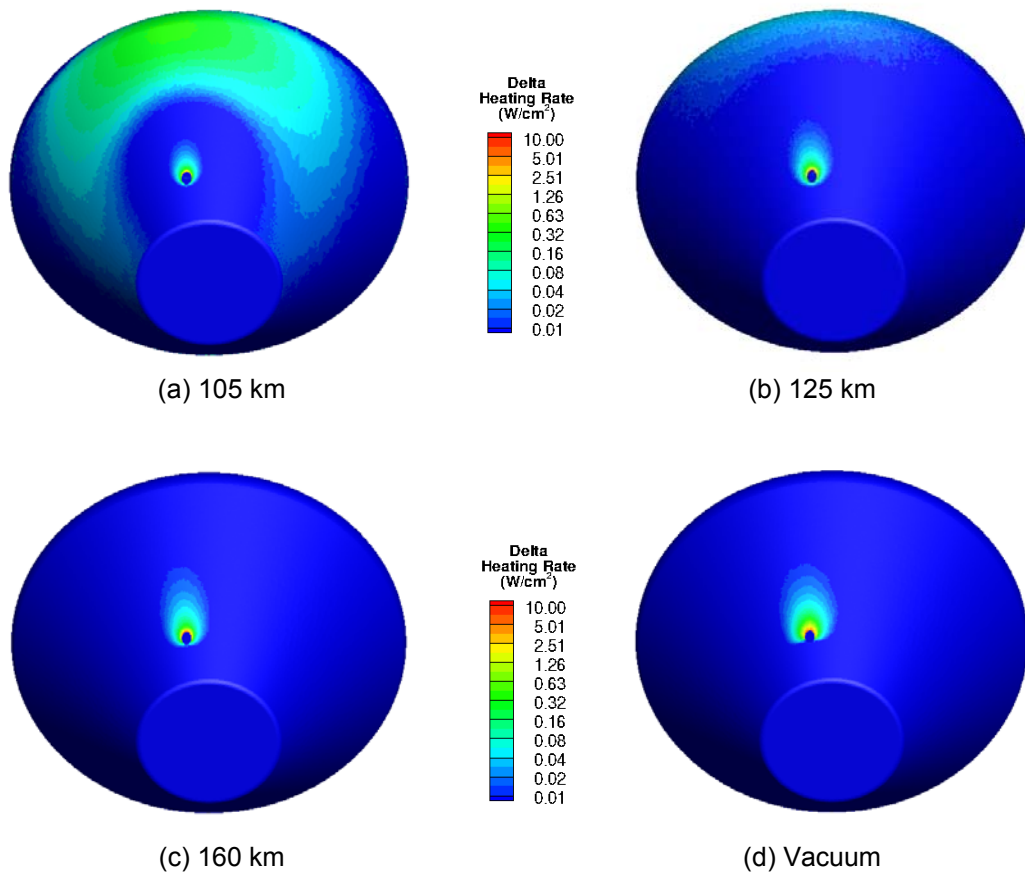


Figure 8. Surface heat rate increase over plume-off solution from the Orion CM pitch-down jet at each free stream condition (a-c) Delta heating (d) Absolute heating.

The JFI surface heating effects have different footprints for each jet as shown in Fig. 9. The plots show the delta increase in heat flux over the plume-off solution on the same scale for each simulated thruster at 105 km. Fig. 9 (a, b, and d) are all in the same orientation. Fig. 9 (c) has been rotated to more clearly show the JFI that occurs for the yaw thruster firing. The plots are ordered (a) through (d) in the order of the severity of the JFI surface heating effects. The roll jet and pitch-down jet are both oriented slightly toward the oncoming free stream, which causes the JFI to be much more severe. While the pitch-down jet causes a larger JFI footprint, the peak



surface heating increase for the roll jet is twice as much as the pitch-down jet because it is located much closer to the vehicle shoulder and the bow shock. Both the pitch-up and yaw thrusters point away from the oncoming free stream and are located close to the vehicle shoulder. The yaw jet however, is located closer to the windward side of the vehicle and thus the interaction with the free stream is more severe.

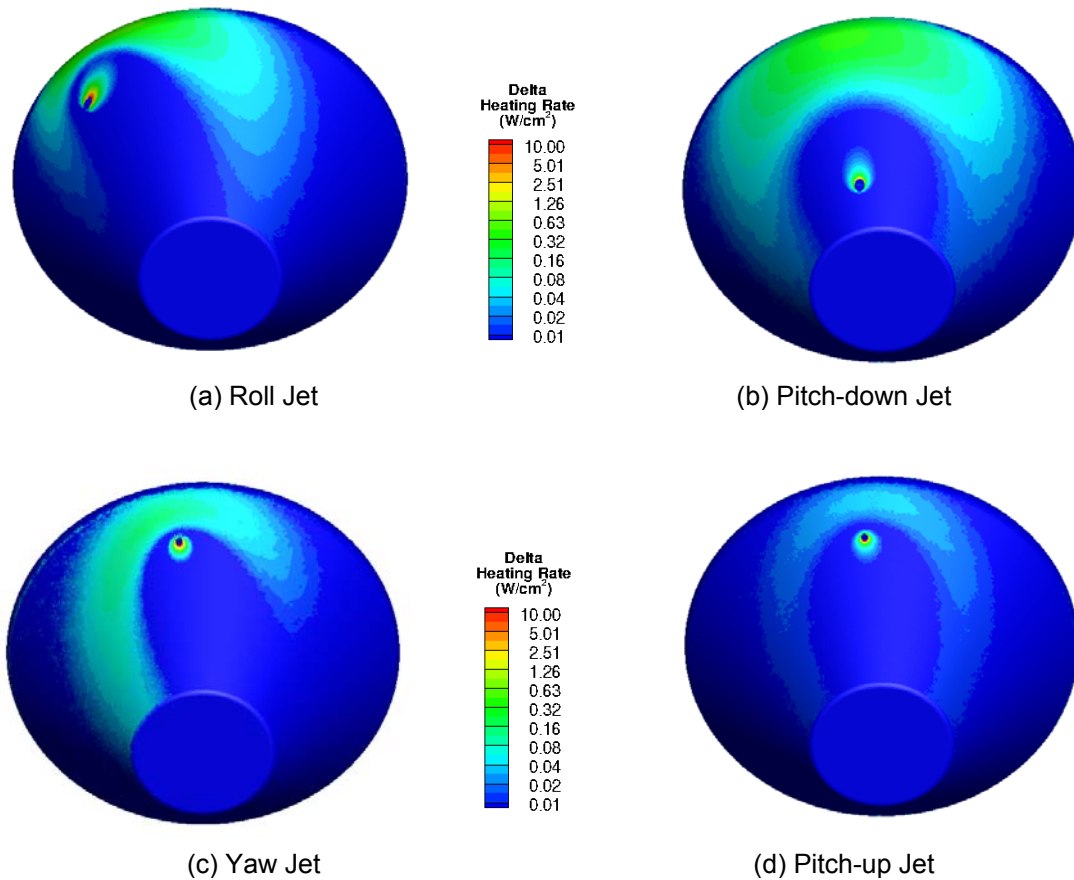
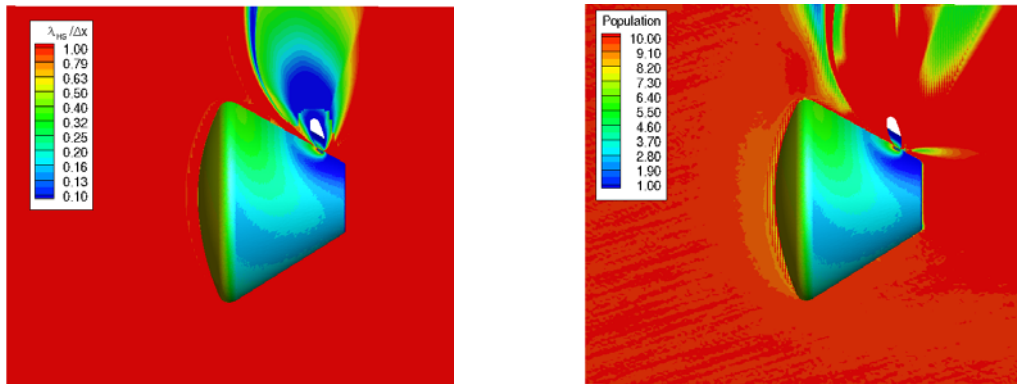


Figure 9. Surface heat rate increase over plume-off solution for each simulated Orion RCS thruster at 105 km altitude.

### SOLUTION QUALITY

The DSMC solution quality is confirmed by investigating cell population and mean free path resolution (MFPR). The MFPR and population for the pitch-down jet firing at 105 km are shown in Fig. 10. For typical DSMC simulations, a MFPR  $\geq 1.0$  and a population  $\geq 6$  are required to have a high confidence solution. Fig. 10 shows that these requirements are met for the majority of the flow field domain. The plots show that the quality of the simulation diminishes near the plume inflow boundary and in the vehicle bow shock/plume boundary shock interaction region. The use of nearest neighbor collision pairs relaxes the MFPR requirement, but the contour values shown in Fig 10. (a) suggest further refinement or a larger plume inflow boundary is necessary to completely meet the standard DSMC requirements.



(a) Mean Free Path Resolution

(b) Population

Figure 10. MFPR and cell population contours plotted with surface heat rate for the Orion CM pitch-down jet

## SUMMARY AND CONCLUSIONS

A CFD/DSMC analysis was performed with the DPLR and DAC codes to capture the interaction heating effects for the reentry of the Orion MPCV CM with active single RCS thruster firings. The roll, yaw, pitch-up and pitch-down jets were investigated at free stream altitudes of 105 km, 125 km, and 160 km, as well as at vacuum conditions. The angle of attack and free stream velocity were kept constant to match the plume-off solutions. The results of the analysis show that the JFI effects increase the heating to the Orion backshell surface, but the overall heating is low (on the order of 1.0 – 2.0 W/cm<sup>2</sup>) and the effects only exist for a limited range of the rarefied portion of the reentry trajectory (160 km and below). Investigation of the solution quality reveals that some of the simulations may need to be further resolved to more closely meet the standard DSMC solution requirements for MFPR and cell population.

## FUTURE WORK

This analysis represents a portion of an on-going effort to characterize and quantify the aerothermodynamics and plume impingement environments for the Orion CM heat shield. The existing simulations will be further refined to increase the MFPR. Further work is planned to investigate dual jet interactions with the free stream for the roll and yaw jets. In addition, the CFD/DSMC simulations will be utilized to assess plume impingement to other space vehicles and hardware from the Orion CM.

## REFERENCES

1. Lee, D. B., Bertin, J. J., and Goodrich, W. D., ***Heat-transfer Rate and Pressure Measurements Obtained During Orbital Entries***, NASA TN-D-6028, NASA Johnson Space Center, (Oct 1970).
2. Lumpkin, F. E., III, Le Beau, G. J., and Stuart, P. C., ***A CFD/DSMC Analysis of Plumes and Plume Impingement during Shuttle/Mir docking***, AIAA Paper No. 95-2034, 30<sup>th</sup> AIAA Thermophysics Conference (Jun 1995).
3. Lumpkin, F. E., III, LeBeau, G. J., and Stuart, P. C., ***An Enhanced Analyses of Plume Impingement During Shuttle-Mir Docking Using a Combined CFD and DSMC Methodology***, AIAA Paper No. 96-1877, 31<sup>st</sup> AIAA Thermophysics Conference (June 1996).

4. Lumpkin, F. E., III and Larin, M. E., ***Simulation of the Plume from the Firing of Four R4D Engines on the H-2 Transfer Vehicle using the GASP and DAC Codes***, 29<sup>th</sup> JANNAF Exhaust Plume Technology Subcommittee Meeting (Jun 2006).
5. Wright, M. J., Candler, G. V. and Bose, D., ***Data-Parallel Line Relaxation Method for Navier-Stokes Equations***, AIAA Journal, Vol. 36, No. 9 (Sep 1998).
6. Bird, G. A., ***Breakdown of Continuum Flow in Free Jets and Rocket Plumes***, 12<sup>th</sup> International Symposium on Rarefied Gas Dynamics, Progress in Aeronautics and Astronautics (1981).
7. LeBeau, G. J. and Lumpkin, F. E., III, ***Application Highlights of the DSMC Analysis Code (DAC) Software for Simulating Rarefied Flows***, Computer Methods in Applied Mechanics and Engineering, 191, No. 6-7, 595-609 (2001).
8. Menter, F. R., ***Two-Equation Eddy-Viscosity Turbulence Models for Engineering Applications***, AIAA Journal, Vol. 32, No. 8, 1994, pp. 1598–1605.
9. Boyles, K.A., ***CEV Simulation Guidelines for the DSMC Analysis Code (DAC) Software***, NASA CAP Document No. EG-CAP-06-145, Version 1.1, March 22, 2007.
10. Boyles, K. A., LeBeau, G. J., Lumpkin, F. E., III, and Blanchard, R. C., ***The Use of Virtual Sub-cells in DSMC Analysis of Orbiter Aerodynamics at High Altitudes Upon Reentry***, AIAA Paper No.2003-1030, 41<sup>st</sup> AIAA Aerospace Sciences Meeting and Exhibit (Jan 2003).